Effects of transverse trapping on the ground state of a cigar-shaped two-component Bose–Einstein condensate*

Cui Guo-Dong(崔国栋)[a)b)], Sun Jian-Fang(孙剑芳)[a)b)], Jiang Bo-Nan(姜伯楠)[a)b)], Qian Jun(钱 军)[a)†], and Wang Yu-Zhu(王育竹)[a)‡]

[a)] *Key Laboratory for Quantum Optics, Center for Cold Atoms, Shanghai Institute of Optics and Fine Mechanics, Chinese Academy of Sciences, Shanghai* 201800, *China*

[b)] *University of Chinese Academy of Sciences, Beijing* 100049, *China*

(Received 23 February 2013; revised manuscript received 3 April 2013)

We derive the coupled nonpolynomial nonlinear Schrödinger equations for a two-component Bose–Einstein condensate in a quasi-one-dimension geometry and investigate the effects of a tightly transverse trapping on the ground state and the miscibility–immiscibility threshold. We find that the density profile of the matter wavepacket is remarkably dependent on the transverse width and the effective one-dimension nonlinear coupling strengths in miscible and immiscible regimes.

Keywords: Boson mixtures, trapped gases, static properties of condensates, transverse trapping

PACS: 67.60.Bc, 67.85.−d, 67.85.Bc **DOI:** 10.1088/1674-1056/22/9/096701

1. Introduction

Since the first realization of Bose–Einstein condensates (BEC) in 1995,[1,2] this field has been intensively studied. Under the mean-field approximation, the Gross–Pitaevskii equation (GPE) has been successfully used to describe the behavior of BECs in free space and traps, and correctly predicts a variety of interesting phenomena such as vortex,[3,4] soliton,[5,6] and disordered quantum gases.[7] Experimentally, a BEC can be produced in a highly anisotropic trap to prepare a low-dimensional quantum gas.[8–11] Then the BEC has a cigar or disk shape, which can be described by a quasi-one-dimension (1D) or two-dimension (2D) effective GPE derived by integrating out the slow degrees of freedom under the adiabatic approximation.[12–15] Taking the transverse trapping effect into account, 1D and 2D nonpolynomial nonlinear Schrödinger equations (NPSE) have been proven to be more exact in the situations where a strong interaction or a dense atomic sample has to be considered.[16]

With rapidly developing experimental techniques, multi-component BECs have been produced with different hyperfine spin states or different atomic species.[17–22] A two-component BEC (tBEC) has more complicated static and dynamical properties compared with the single-component BEC due to the additional inter-component nonlinear coupling. One of the most important phenomena is phase separation, which has been observed unambiguously.[20,21] Depending on the strength of the inter-component atomic interaction, the tBEC can experience a miscibility–immiscibility transition, which can be used as a prototypical platform for the investigation of critical phenomena due to the unprecedented experimental control of relevant parameters. So far, similar to the single-component BEC, the coupled GPEs have been widely applied to investigate the wavefunction at zero temperature and the transport of matter wavepackets.[23–29] Subsequently, the coupled NPSEs are introduced to improve the GPEs, especially in the situation of strong interaction or dense gas, by considering the transverse confinement more exactly.[30,31]

In this work, we compare the ground state of the tBEC obtained by numerically solving the GPEs and NPSEs in the miscible and immiscible regimes respectively. It is found that, although both models grasp the physics of phase separation, they predict different density profiles of the ground state and different miscibility–immiscibility thresholds as a result of the transverse trapping. We also find inhomogeneous transverse widths and effective 1D nonlinear coupling strengths in the NPSEs, while they are constant presented in the GPEs. In turn, the density-dependent transverse widths have a dramatic effect on the ground state obtained in the tBEC.

2. Theoretical model

We consider a two-component BEC with two hyperfine states of the atom in a trap. By exerting a magnetic bias field to counteract the gravitation, a highly anisotropic external harmonic oscillator potential with an axial symmetry can be written as follows:

$$V(x,y,z) = \frac{1}{2}m\omega_\perp^2\left(x^2+y^2+\lambda^2 z^2\right), \tag{1}$$

*Project supported by the National Natural Science Foundation of China (Grant No. 11104292) and the National Basic Research Program of China (Grant No. 2011CB921504).

†Corresponding author. E-mail: jqian@siom.ac.cn

‡Corresponding author. E-mail: yzwang@mail.shcnc.ac.cn

© 2013 Chinese Physical Society and IOP Publishing Ltd

where $\omega_\perp$ and ω_z are the transverse and axial trap frequencies, respectively, and $\lambda = \omega_z/\omega_\perp$ is the aspect ratio of the trap, which characterizes the anisotropy of the trap. The BEC has a cigar shape for $\lambda < 1$, and a disk shape for $\lambda > 1$. In this work, we focus on the situation with $\lambda \ll 1$,[8,9] so the dynamics of the tBEC is only allowed to develop in the axial direction and its motion degrees of freedom in the transverse direction are frozen. Because the system's evolution in the axial direction is faster than the transverse one, we can concentrate on the tBEC's property in the axial direction. Integrating along the transverse coordinates, we arrive at dimensionless effective 1D GPEs for the axial wave functions $\varphi_{\rm A}(z)$ and $\varphi_{\rm B}(z)$[26,27]

$$\begin{aligned} \mathrm{i}\frac{\partial \varphi_{\rm A}}{\partial t} &= \left(-\frac{1}{2}\frac{\partial^2}{\partial z^2} + \frac{1}{2}\lambda^2 z^2 + U_{\rm AA}|\varphi_{\rm A}|^2 + U_{\rm AB}|\varphi_{\rm B}|^2\right)\varphi_{\rm A}, \\ \mathrm{i}\frac{\partial \varphi_{\rm B}}{\partial t} &= \left(-\frac{1}{2}\frac{\partial^2}{\partial z^2} + \frac{1}{2}\lambda^2 z^2 + U_{\rm BB}|\varphi_{\rm B}|^2 + U_{\rm AB}|\varphi_{\rm A}|^2\right)\varphi_{\rm B}, \end{aligned} \quad (2)$$

where dimensionless effective 1D interaction strengths $U_{ii} = 2Na_{ii}/b_\perp$ $(i = {\rm A}, {\rm B})$ and $U_{\rm AB} = 2Na_{\rm AB}/b_\perp$ are characterized by intra- and inter-component scattering lengths a_{ii} and $a_{\rm AB}$, respectively. The dimensionless units of length, time, and energy are $b_\perp = \sqrt{\hbar/m\omega_\perp}$, $\omega_\perp^{-1}$, and $\hbar\omega_\perp$, respectively. In addition, the density of each component is normalized to the ratio of its atomic number to the total number N.

Now we follow the routine of Salasnich *et al.*[16,30,31] to derive the 1D effective coupled NPSEs, which have been demonstrated as an exact model especially for the case with a dense gas or a strong mutual-atom interaction. In our treatment, it is different from the GPEs in that the transverse width $\sigma_i(z,t)$ is treated as a slow variable compared to the change of the axial wavefunction. By taking wavefunction complex conjugation φ_i^* and transverse width σ_i as variables, the Euler–Lagrange equations, i.e. the so called effective 1D NPSEs, are written as

$$\begin{aligned} \mathrm{i}\frac{\partial \varphi_{\rm A}}{\partial t} &= \Big(-\frac{1}{2}\frac{\partial^2}{\partial z^2} + \frac{1}{2}\lambda^2 z^2 + U'_{\rm AA}|\varphi_{\rm A}|^2 + U'_{\rm AB}|\varphi_{\rm B}|^2 \\ &\quad + \frac{1}{2}\frac{1}{\sigma_{\rm A}^2} + \frac{1}{2}\sigma_{\rm A}^2\Big)\varphi_{\rm A}, \\ \mathrm{i}\frac{\partial \varphi_{\rm B}}{\partial t} &= \Big(-\frac{1}{2}\frac{\partial^2}{\partial z^2} + \frac{1}{2}\lambda^2 z^2 + U'_{\rm BB}|\varphi_{\rm B}|^2 + U'_{\rm AB}|\varphi_{\rm B}|^2 \\ &\quad + \frac{1}{2}\frac{1}{\sigma_{\rm B}^2} + \frac{1}{2}\sigma_{\rm B}^2\Big)\varphi_{\rm B}, \end{aligned} \quad (3)$$

where

$$\begin{aligned} \sigma_{\rm A}^4 &= \sigma_{\rm A0}^4 + 4U'_{\rm AB}\frac{\sigma_{\rm A}^4}{\sigma_{\rm A}^2 + \sigma_{\rm B}^2}|\varphi_{\rm B}|^2, \\ \sigma_{\rm B}^4 &= \sigma_{\rm B0}^4 + 4U'_{\rm AB}\frac{\sigma_{\rm B}^4}{\sigma_{\rm A}^2 + \sigma_{\rm B}^2}|\varphi_{\rm A}|^2, \end{aligned} \quad (4)$$

with the dimensionless effective 1D nonlinear coupling strengths $U'_{ii} = 2Na_{ii}/(\sigma_i^2 b_\perp)$ and $U'_{\rm AB} = 2Na_{\rm AB}/[(\sigma_{\rm A}^2 + \sigma_{\rm B}^2)b_\perp]$. Here $\sigma_{i0} = (1 + U'^2_{ii}\sigma_i^2|\varphi_i|^2)^{1/4}$ is the transverse width due to the intra-component interaction which has been obtained in the single-component 1D NPSE.[16] Obviously, the above NPSEs explicitly show the complicated relations among the atomic density distribution, the transverse trapping, and the nonlinear couplings. One can observe that, in the weakly interacting limit, the above NPSEs (Eq. (3)) can be reduced to the familiar GPEs (Eq. (2)) as $\sigma_i = b_\perp$. In addition, the inter- and intra-component nonlinear coupling strengths are also dependent on the corresponding transverse widths. In turn, it is clearly shown in Eq. (4) that the transverse widths are dependent on the density. Thus it is very difficult to elaborate the influence of the above correction analytically.

3. Numerical results and discussion

Below we first numerically solve Eqs. (2) and (3) by propagating an initial trial wavefunction with the split-step spectral algorithm in imaginary time.[32] Taking account of the transverse trapping effect, we update the transverse widths (Eq. (4)) at each time step. In the simulation, we adopt the experimental data measured by Nicklas *et al.*,[33] they have prepared a tBEC close to the miscibility–immiscibility threshold with a balanced mixture of two hyperfine levels of ^{87}Rb ($N_{\rm A} = N_{\rm B} = 2200$). The axial and transverse trap frequencies are $\omega_z = 2\pi \times 22$ Hz and $\omega_\perp = 2\pi \times 460$ Hz, respectively. The scattering lengths are $a_{\rm AA} = 95a_0$ and $a_{\rm BB} = 100.4a_0$, where a_0 is the Bohr radius, whereas $a_{\rm AB}$ can be tuned by the Feshbach resonance, which can bring the tBEC into different parameter regimes.[34–36]

The main results are shown in Fig. 1, which depicts the ground states of the tBEC in the miscible and immiscible regimes. In the miscible regime, the overlap between the wavefunctions of the two components is very large, while the wavefunctions are separated (or immiscible) in space in the opposite limit. With given intra-component interaction strengths, the phase of the system is only dependent on the inter-component interaction strength and the GPEs predict that there is a miscibility–immiscibility threshold $a_{\rm AB} = \sqrt{a_{\rm AA}a_{\rm BB}}$ as shown in Figs. 1(a) and 1(b). However, we cannot obtain the same threshold from the NPSEs because the separation between the two components is not clear in this case (see the red dashed line in the middle panel in Fig. 1(b)). Since the NPSEs differ from the GPEs with the correction of the transverse trapping, we can conclude that the tightly transverse trapping has a remarkable influence on the density profile of the condensate. Concretely, in the miscible limit ($a_{\rm AB} < \sqrt{a_{\rm AA}a_{\rm BB}}$), the axial widths of the ground states derived from the NPSEs are much narrower than those obtained from the GPEs. In the immiscible regime ($a_{\rm AB} > \sqrt{a_{\rm AA}a_{\rm BB}}$), however, the NPSEs predict that more atoms of component A occupy the center and the boundary between the two components is much closer to the center than that calculated in the GPEs. Quantitatively, we introduce the central fraction of component B ($C_{\rm B}$) and the overlap between the two components

($f = \int\langle\varphi_A|\varphi_B\rangle dz/\int\langle\varphi_A|\varphi_A\rangle dz$) to describe the phase separation of the tBEC in detail, as also shown in Figs. 1(c) and 1(d).

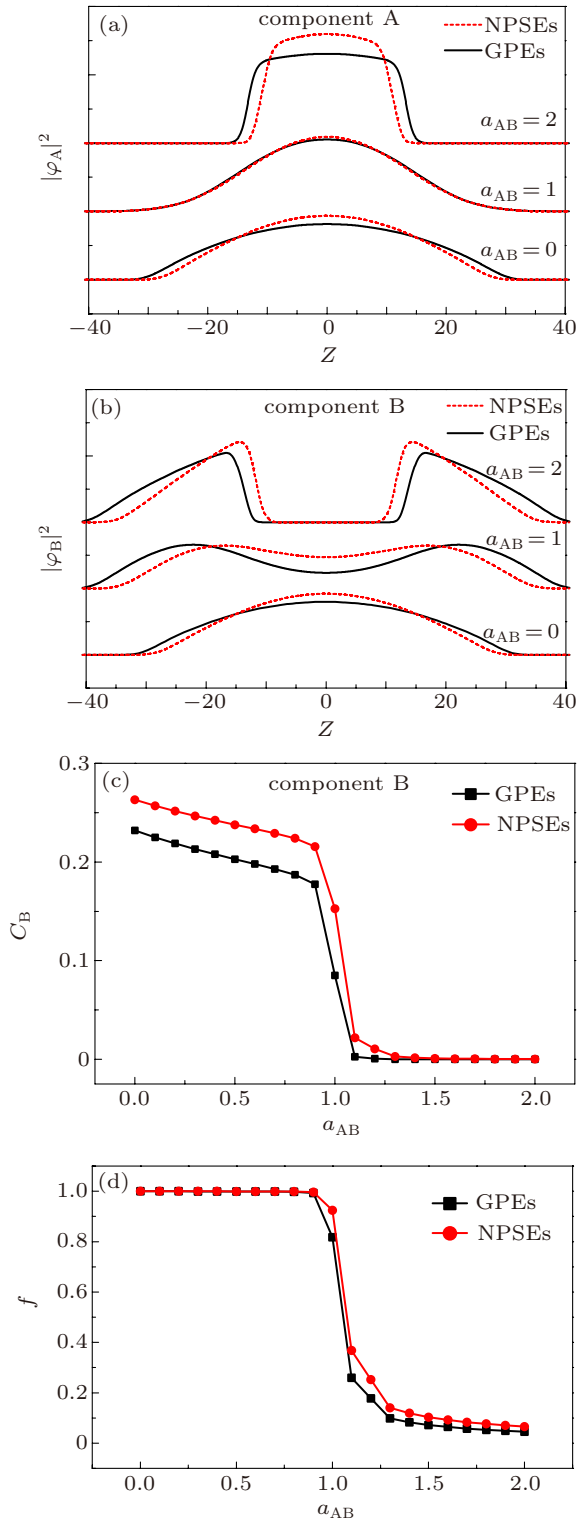


Fig. 1. (color online) Axial density profiles of (a) component A and (b) component B derived from the GPEs (black solid) and NPSEs (red dashed) for different inter-component interaction strengths. The scattering lengths $a_{AA} = 95a_0$ and $a_{BB} = 100.4a_0$ are fixed, and a_{AB} is scaled by $\sqrt{a_{AA}a_{BB}}$. (c) Central fraction of component B (C_B) in $z \in [-10, 10]$. (d) Overlap of the two component wavefunctions $f = \int\langle\varphi_A|\varphi_B\rangle dz/\int\langle\varphi_A|\varphi_A\rangle dz$, where red circles and black squares are the results from the NPSEs and GPEs, respectively.

Intuitively, the phase separation is expected to be associated with the reduction of central fraction C_B and overlap f, especially when they approach zero. In Figs. 1(c) and 1(d), both C_B and f change moderately when the components are miscible or immiscible, however, there is a sudden drop across the miscibility–immiscibility transition ($a_{AB} \sim \sqrt{a_{AA}a_{BB}}$). The GPEs and NPSEs agree with each other well in this sense. But we can find that the two models predict different critical values of a_{AB} when the separation happens. For example, at the threshold $a_{AB}/\sqrt{a_{AA}a_{BB}} = 1$ given by the GPEs, C_B approaches to 0.08 in the GPEs and 0.15 in the NPSEs. Similarly, f goes down to 0.80 in the GPEs but 0.97 in the NPSEs. It is clear that the NPSEs predict a larger threshold of the miscibility–immiscibility crossover than the GPEs due to the correction of the transverse trapping.

In the above discussion, we have demonstrated that the transverse trapping has a remarkable influence on the density profile of the tBEC and thus obviously changes the dependence of the miscibility–immiscibility threshold on a_{AB}. Now we can investigate the physical origin of this effect. As Eq. (4) shows, the transverse widths are temporal- and spacial-dependent in the NPSEs rather than constants in the GPEs. Both intra- and inter-component interactions will contribute to the modification of the transverse width, while the former depends on the density distribution of one component itself and the latter is related to the density profile of the other one. Hence, the situation becomes a bit more complicated because the density profile and the transverse width are greatly interdependent. In Fig. 2, inhomogeneous transverse widths of both components are given for several typical cases. For a miscible quantum mixture, $\sigma_{A,B}$ are like inverted parabolas and become wider and wider when a_{AB} increases. It can be easily understood because the wavefunctions overlap and coexist in the center of the trap, that is to say, the density profiles are similar to the inverted parabolas. Thus, the two terms in the right side of Eq. (4) should share the same shape, which illustrates that the shapes of σ_A and σ_B are similar. However, once the system enters into the immiscible regime, a two-dump envelop appears for σ_A, and simultaneously a raised plateau emerges in the center for σ_B. Qualitatively, in this situation, the atoms of component A still gather around the center of the trap, while those of component B spread outwards along the axial direction. Therefore, it is indicated in Eq. (4) that the transverse widths display different shapes. In addition, we also find another interesting result that σ_A is almost unchanged in the central zone whatever a_{AB} is. This is because the contributions from the two terms to σ_A are nearly canceled out in the central zone. We can also find the support for the aforementioned

results in Fig. 2(c), where the widths $\sigma_{A,B}$ at the origin $z = 0$ are shown. Evidently, both $\sigma_A(0)$ and $\sigma_B(0)$ increase slightly in the miscible regime. In the immiscible regime, however, $\sigma_A(0)$ approximately remains unchanged and $\sigma_B(0)$ increases markedly when a_{AB} becomes large enough, which is in good agreement with the rising plateau in Fig. 2(b).

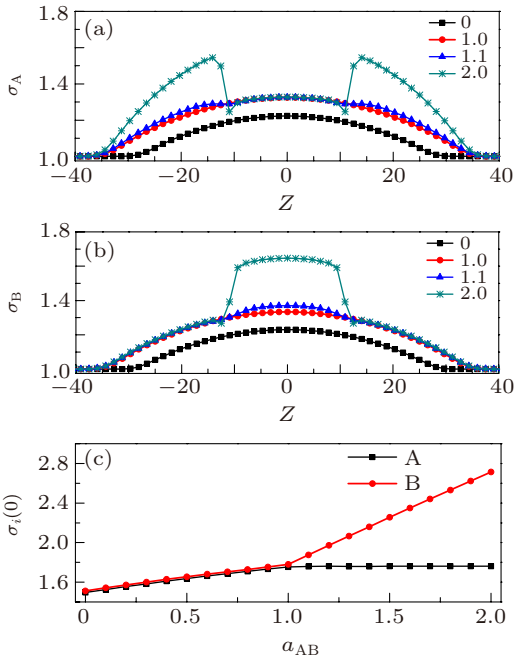


Fig. 2. (color online) Inhomogeneous transverse widths of (a) component A and (b) component B for $a_{AB}/\sqrt{a_{AA}a_{BB}} = 0$ (black squares), 1 (red circles), 1.1 (blue triangles), 2 (dark cyan stars). (c) Transverse width at $z = 0$. Components A and B are labeled by black squares and red circles, respectively.

As predicted by the NPSEs, the modification of the ground state of the tBEC originates from the transverse trapping, and the effect cannot be ignored especially when the effective 1D nonlinear coupling strength between the components is strong enough. Below we will demonstrate that the inhomogeneous distribution of the transverse width reflects the fact that the effective 1D nonlinear coupling strengths are also inhomogeneous. As shown in Fig. 3, we pay special attention to U'_{AA}, U'_{BB}, and U'_{AB} that are all related to the density profiles of the condensates. Since U'_{AA} and U'_{BB} are inversely proportional to the squares of their respective transverse widths, we can easily obtain them from Figs. 2(a) and 2(b). For a strong inter-component interaction, it is clearly depicted in Fig. 3(a) that U'_{AA} is convex and U'_{BB} is concave in the center. The situation becomes quit different for U'_{AB} when two peaks present in the background of a parabola. It can be explained based on the expression of $U'_{AB} \sim (\sigma_A^2 + \sigma_B^2)^{-1}$, a local maximum can be reached at $z \simeq \pm 10$ where the sum of σ_A^2 and σ_B^2 becomes minimum.

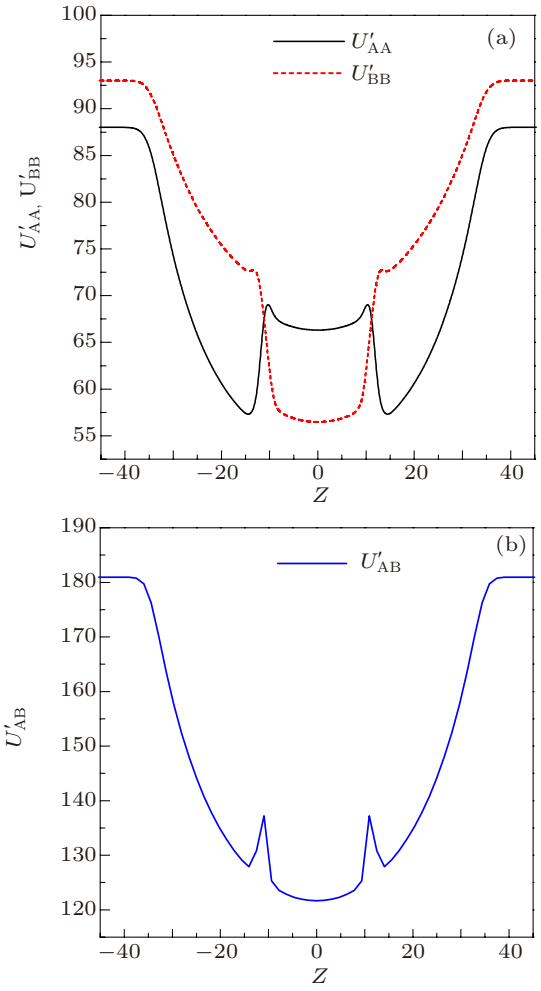


Fig. 3. (color online) Effective 1D nonlinear coupling strengths for an immiscible bosonic mixture: (a) U'_{AA} and U'_{BB}, (b) U'_{AB}. The scattering lengths are $a_{AA} = 95.0a_0$, $a_{BB} = 100.4a_0$, and $a_{AB} = 2\sqrt{a_{AA}a_{BB}}$.

4. Conclusion

In summary, we have derived the effective 1D NPSEs for the tBEC trapped tightly in the transverse direction and highlighted the effects of the transverse trapping on the ground state of the condensates. We have demonstrated that in the limit of strong interaction or dense gases, the NPSEs predict a larger threshold of the miscibility–immiscibility transition than the GPEs. The inhomogeneity of the transverse width and the effective 1D nonlinear coupling have been also studied in detail. The results presented here are expected to be relevant to experiments realizable in the near future.

References

[1] Davis K B, Mewes M O, Andrews M R, van Druten N J, Durfee D S, Kurn D M and Ketterle W 1995 *Phys. Rev. Lett.* **75** 3969

[2] Anderson M H, Ensher J R, Matthews M R, Wieman C E and Cornell E A 1995 *Science* **269** 198

[3] Matthews M R, Anderson B P, Haljan P C, Hall D S, Wieman C E and Cornell E A 1999 *Phys. Rev. Lett.* **83** 2498

[4] Madison K W, Chevy F, Wohlleben W and Dalibard J 2000 *Phys. Rev. Lett.* **84** 806

[5] Khaykovich L, Schreck F, Ferrari G, Bourdel T, Cubizolles J, Carr L D, Castin Y and Salomon C 2002 *Science* **296** 1290

[6] Strecker K E, Partridge G B, Truscott A G and Hulet R G 2002 *Nature* **417** 150

[7] Sanchez-Palencia L and Lewenstein M 2010 *Nature Phys.* **6** 87

[8] Mewes M O, Andrews M R, Van Druten N J, Kurn D M, Durfee D S and Ketterle W 1996 *Phys. Rev. Lett.* **77** 416

[9] Görlitz A, Vogels J M, Leanhardt A E, Raman C, Gustavson T L, Abo-Shaeer J R, Chikkatur A P, Gupta S, Inouye S, Rosenband T and Ketterle W 2001 *Phys. Rev. Lett.* **87** 130402

[10] Greiner M, Bloch I, Mandel O, Hänsch T W and Esslinger T 2001 *Phys. Rev. Lett.* **87** 160405

[11] Schreck F, Khaykovich L, Corwin K L, Ferrari G, Bourdel T, Cubizolles J and Salomon C 2001 *Phys. Rev. Lett.* **87** 080403

[12] Mateo A M and Delgado V 2008 *Phys. Rev. A* **77** 013617

[13] Kamchatnov A M and Shchesnovich V S 2004 *Phys. Rev. A* **70** 023604

[14] Massignan P and Modugno M 2003 *Phys. Rev. A* **67** 023614

[15] Jackson A D, Kavoulakis G M and Pethick C J 1998 *Phys. Rev. A* **58** 2417

[16] Salasnich L, Parola A and Reatto L 2002 *Phys. Rev. A* **65** 043614

[17] Myatt C J, Burt E A, Ghrist R W, Cornell E A and Wieman C E 1997 *Phys. Rev. Lett.* **78** 586

[18] Mertes K M, Merrill J W, Carretero-González R, Frantzeskakis D J, Kevrekidis P G and Hall D S 2007 *Phys. Rev. Lett.* **99** 190402

[19] Thalhammer G, Barontini G, De Sarlo L, Catani J, Minardi F and Inguscio M 2008 *Phys. Rev. Lett.* **100** 210402

[20] Modugno G, Modugno M, Riboli F, Roati G and Inguscio M 2002 *Phys. Rev. Lett.* **89** 190404

[21] Papp S B, Pino J M and Wieman C E 2008 *Phys. Rev. Lett.* **101** 040402

[22] Ma X Q, Chen S, Yang F, Xia L, Zhou X J, Wang Y Q and Chen X Z 2005 *Chin. Phys. Lett.* **22** 5

[23] Ho T L and Shenoy V B 1996 *Phys. Rev. Lett.* **77** 3276

[24] Pu H and Bigelow N P 1998 *Phys. Rev. Lett.* **80** 1130

[25] Adhikari S K 2001 *Phys. Rev. E* **63** 056704

[26] Wang D S, Hu X H and Liu W M 2010 *Phys. Rev. A* **82** 023612

[27] Kasamatsu K and Tsubota M 2006 *Phys. Rev. A* **74** 013617

[28] Yan J R and Zhou J 2012 *Chin. Phys. B* **21** 060304

[29] Wang Q, Wen L and Li Z D 2013 *Chin. Phys. B* **22** 080501

[30] Salasnich L and Malomed B A 2006 *Phys. Rev. A* **74** 053610

[31] Salasnich L, Malomed B A and Toigo F 2008 *Phys. Rev. A* **77** 035601

[32] Press W H, Teukolsky S A, Vetterling W T and Flannery B P 2007 *Numerical Recipes* (3rd edn.) (New York: Cambridge University Press)

[33] Nicklas E, Strobel H, Zibold T, Gross C, Malomed B A, Kevrekidis P G and Oberthaler M K 2011 *Phys. Rev. Lett.* **107** 193001

[34] Widera A, Mandel O,Greiner M, Kreim S, Hänsch T W and Bloch I 2004 *Phys. Rev. Lett.* **92** 160406

[35] Erhard M, Schmaljohann H, Kronjäger J, Bongs K and Sengstock K 2004 *Phys. Rev. A* **69** 032705

[36] Chin C, Grimm R, Julienne P and Tiesinga E 2010 *Rev. Mod. Phys.* **82** 1225